

Resonant two-magnon Raman scattering in cuprate antiferromagnetic insulators

G. Blumberg

*National Science Foundation, Science and Technology Center for Superconductivity and
Department of Physics, University of Illinois at Urbana-Champaign, Urbana, Illinois 61801-3080
and Institute of Chemical Physics and Biophysics, R vala 10, Tallinn EE0001, Estonia*

P. Abbamonte, M. V. Klein, W. C. Lee,* and D. M. Ginsberg

*National Science Foundation, Science and Technology Center for Superconductivity and
Department of Physics, University of Illinois at Urbana-Champaign, Urbana, Illinois 61801-3080*

L. L. Miller

Ames Laboratory, Iowa State University, Ames, Iowa 50011

A. Zibold

Department of Physics, University of Florida, Gainesville, Florida 32611

(Received 20 February 1996)

We present results of low-temperature two-magnon resonance Raman excitation profile measurements for single-layer $\text{Sr}_2\text{CuO}_2\text{Cl}_2$ and bilayer $\text{YBa}_2\text{Cu}_3\text{O}_{6+\delta}$ antiferromagnets over the excitation region from 1.65 to 3.05 eV. These data reveal composite structure of the two-magnon line shape and strong nonmonotonic dependence of the scattering intensity on excitation energy. We analyze these data using the *triple resonance* theory of Chubukov and Frenkel [Phys. Rev. Lett. **74**, 3057 (1995)] and deduce information about magnetic interaction and band parameters in these materials. [S0163-1829(96)50618-1]

The insulating phases of the high- T_c materials are antiferromagnets (AF) with spin $\mathbf{S}=\frac{1}{2}$, localized on Cu atoms of the CuO_2 planes, characterized by superexchange constant $J\approx 120$ meV and a N el temperature $T_N\approx 300$ K.^{1,2} The magnetic interactions in the CuO_2 planes can be described by a Heisenberg Hamiltonian on the two-dimensional (2D) square lattice $H=J\sum_{\langle i,j\rangle}(\mathbf{S}_i\cdot\mathbf{S}_j-\frac{1}{4})$, where \mathbf{S}_i is the spin on site i and the summation is over nearest-neighbor Cu pairs.

Two-magnon (2M) Raman scattering (RS) probes mainly short wavelength magnetic excitations in the AF lattice. The scattering process involves a photon stimulated virtual charge-transfer excitation that exchanges two spins.³ This excitation is also the process that produces the superexchange constant J . Use of photon energies in resonance with the charge-transfer band excitations in a 2M RS study will provide microscopic information on the copper spin superexchange mechanism through oxygen sites that yields the AF interaction.

The traditional Hamiltonian for describing the interaction of light with spin degrees of freedom is the Loudon-Fleury Hamiltonian (Ref. 4), $H=\alpha\sum_{\langle i,j\rangle}(\hat{\mathbf{e}}_i\cdot\mathbf{R}_{ij})(\hat{\mathbf{e}}_j\cdot\mathbf{R}_{ij})\mathbf{S}_i\cdot\mathbf{S}_j$, where $\hat{\mathbf{e}}_i$ and $\hat{\mathbf{e}}_j$ are the polarization vectors of incoming and outgoing photons, α is the coupling constant, and \mathbf{R}_{ij} is a vector connecting two nearest-neighbor sites i and j . Shastry and Shraiman³ have derived this Hamiltonian in the large- U Hubbard model approach for excitation energy below that of the charge-transfer energy. Including final state interactions in this 2M RS theory results in a peak with Raman frequency shift ω near $2.7-2.8J$ in B_{1g} scattering geometry for a single layer 2D lattice of D_{4h} symmetry.⁵⁻⁸ This allows one to determine the exchange interaction constant J directly

from the peak energy observed in the RS spectrum, and, in fact, the Raman data yielded an estimate of J in various cuprates.⁹⁻¹⁸

The dependence of 2M scattering intensity on the incoming excitation energy ω_i has been determined previously over a limited range:¹⁸⁻²⁶ The 2M scattering was very weak for ω_i near the conductivity peak that marks the onset of particle-hole excitation across the charge transfer gap (CTG), scattering increased substantially with ω_i above the CTG. The puzzling lack of resonance at the onset of the CTG prompted the present work. The goal of this comprehensive study is to clarify quantitatively the resonance behavior and to gain insight into the microscopic mechanism of the spin superexchange.

In this paper we report low-temperature two-magnon resonance Raman excitation profile (RREP) measurements for single CuO_2 layer $\text{Sr}_2\text{CuO}_2\text{Cl}_2$ and bilayer $\text{YBa}_2\text{Cu}_3\text{O}_{6+\delta}$ AF insulators, covering the broad excitation region from 1.65 to 3.05 eV. These data reveal composite structure of the 2M line shape and strong nonmonotonic dependence of the shape and 2M scattering intensity on the excitation energy ω_i . We analyze these results within the framework of the Chubukov-Frenkel approach,^{8,27} show that *triple resonance* is the leading process for resonant magnetic RS, and extract microscopic information about the charge transfer band and magnetic interactions in these cuprates.

The investigations were performed on single crystals grown as described in Refs. 28 and 29. Spectra reported here were excited with different Ar^+ , Kr^+ , and dye laser lines in $x'y'$, $x'x'$, xy , and xx pseudo-back-scattering geometries from an [001] crystal face. With assumed D_{4h} symmetry,

this gives RS spectra of $B_{1g}+A_{2g}$, $A_{1g}+B_{2g}$, $B_{2g}+A_{2g}$, and $B_{1g}+A_{1g}$ symmetry, respectively. The A_{2g} component in the 2M excitation region is known to be quite weak.¹² The single crystals were mounted in a continuous helium flow optical cryostat and kept at 5 K. Less than 15 mW of the incident laser power was focused in a 50- μm -diameter spot on the ab -plane crystal surface. The experimental setup and the all spectral corrections made to the frequency dependence of collection optics and spectrometer, detector sensitivity, as well as the optical corrections for transmission coefficients for the incident and scattered photons, their absorption and reabsorption and the scattered photons solid angle correction are described in Ref. 18. The optical parameters were acquired from polarized reflectivity and ellipsometry measurements: we have used the 80 K optical data from Refs. 30 and 31.

The Raman spectra excited with photon energies between 1.9 and 3.1 eV in $x'y'$ and $x'x'$ geometries are shown in Fig. 1. The 2M RS signal sits on a tail of nearly unpolarized photoluminescence background that gets stronger towards lower energies and is peaked in IR.^{18,32} The 2M line shape analyses and the spectra for different polarization have been employed to extract the dependence of the B_{1g} 2M peak intensity on the excitation energy shown in Fig. 2.

The features of primary interest are the following:

(a) Resonant magnetic RS gives the main contribution in the B_{1g} channel. However, as first shown by Sulewski *et al.*,¹² it contributes to the A_{1g} and B_{2g} scattering geometries as well. For these geometries RS bands are broad and have less structure. The A_{1g} intensity is weaker than in the B_{1g} channel, and the B_{2g} intensity is weaker than A_{1g} .

(b) In the B_{1g} channel the 2M band is composite and contains two asymmetric line shapes. $\text{Sr}_2\text{CuO}_2\text{Cl}_2$ shows a band with peaks at 2970 and 3900 cm^{-1} , where the second peak is well resolved for certain excitation energies. For $\text{YBa}_2\text{Cu}_3\text{O}_{6+\delta}$ the 2M band is peaked at 2720 cm^{-1} , and the second peak at 3660 cm^{-1} is resolved only for the lower excitation energies. The 2M band becomes much broader and more symmetric when the excitation energy approaches 3 eV.

(c) In the A_{1g} channel for $\text{Sr}_2\text{CuO}_2\text{Cl}_2$ the 2M band intensity at lower frequencies is a combination of a linear and a cubic power law. For $\text{YBa}_2\text{Cu}_3\text{O}_{6+\delta}$ the 2M band intensity has a flat low-frequency tail and a threshold at about 1750 cm^{-1} . The sharp peaks at the low-energy tails are due to resonant multiphonon scattering that becomes strongly enhanced for excitations closed to the CTG energy.

(d) The 2M scattering intensity strongly depends on the incoming photon energy. For $\text{YBa}_2\text{Cu}_3\text{O}_{6+\delta}$ the B_{1g} peak intensity at 2720 cm^{-1} is enhanced by three orders of magnitude when the excitation approaches 3 eV, that is about 1.3 eV higher than the first peak in ϵ_2 (see Fig. 2), and a weaker resonance is observed at about 2.1 eV, ~ 0.32 eV higher than the peak in ϵ_2 . For $\text{Sr}_2\text{CuO}_2\text{Cl}_2$ the RREP at 2970 cm^{-1} shows resonance at 2.4 eV, about 0.44 eV higher than the ϵ_2 peak at 1.95 eV, and a steep rise to the second strong resonance in the UV region, outside the accessibility of our experimental technique.

These results can be understood in terms of the 2M resonant RS theory proposed by Chubukov and Frenkel^{8,27} that

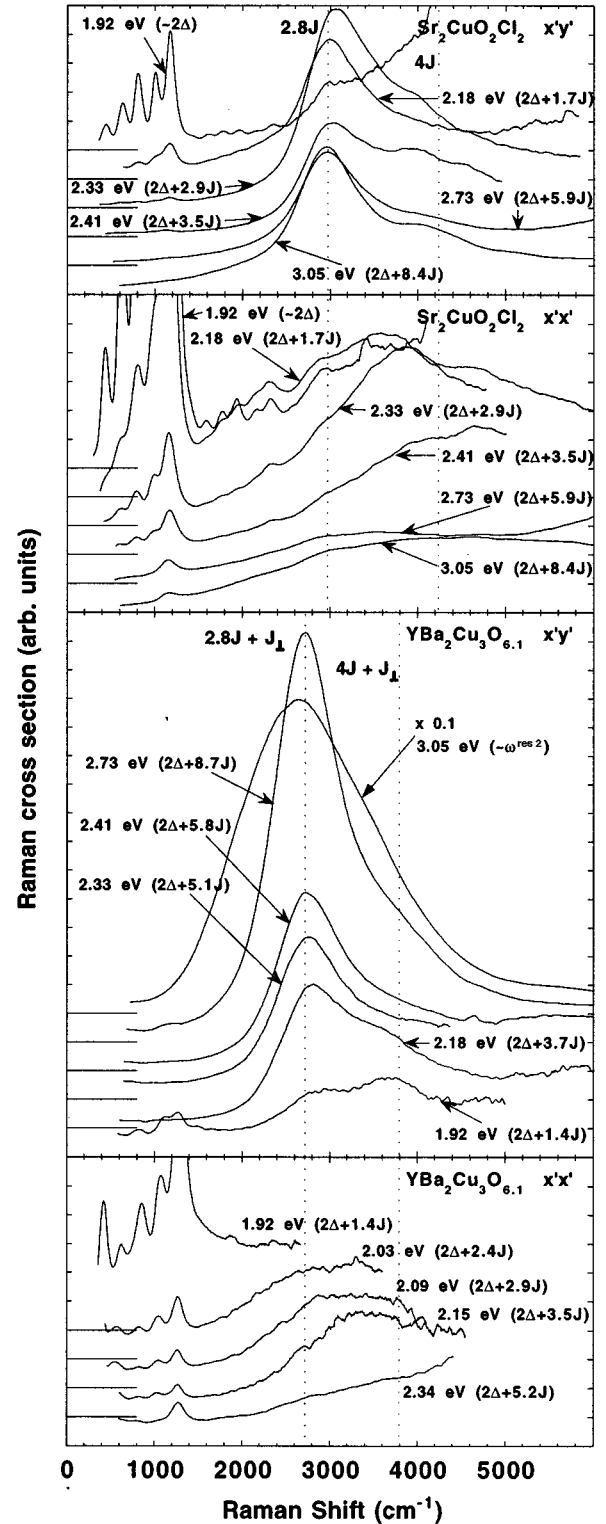


FIG. 1. The two-magnon resonance Raman scattering cross sections ($x'y'$ and $x'x'$ geometries) for $\text{Sr}_2\text{CuO}_2\text{Cl}_2$ and $\text{YBa}_2\text{Cu}_3\text{O}_{6+\delta}$ single crystals for different excitation energies above the charge transfer gap 2Δ . The scattering intensities for $\text{Sr}_2\text{CuO}_2\text{Cl}_2$ are reduced by a factor of 10 relative to $\text{YBa}_2\text{Cu}_3\text{O}_{6+\delta}$. Baselines are shifted as indicated. Dashed lines mark $2.8J+J_{\perp}$ and $4J+J_{\perp}$ Raman shifts. $J_{\text{SCOC}}=1060 \text{ cm}^{-1}$, $J_{\text{YBCO}}=895 \text{ cm}^{-1}$, $J_{\perp\text{SCOC}}=0$, $J_{\perp\text{YBCO}}=215 \text{ cm}^{-1}$.

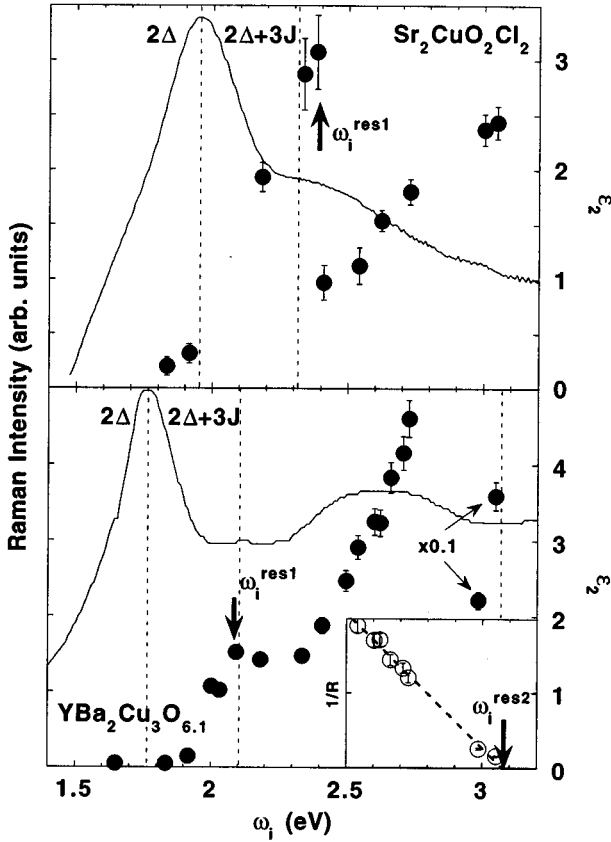


FIG. 2. The intensity of the B_{1g} two-magnon peak at $2.8J$ (circles) as a function of the excitation energy ω_i . Also shown is the imaginary part of the dielectric constant from Refs. 30,31 (solid line). Dashed lines mark the charge transfer gap energy 2Δ and $2\Delta + 3J$. Arrows indicate the *triple resonance* excitation energies. The inset shows the linear fit (dashed line) to the inverse two-magnon peak intensity (open circles).

suggests a leading resonant RS diagram that is different from those leading to the Loudon-Fleury theory. The proposed process is the following: the incoming photon ω_i creates a virtual electron-hole state consisting of an excitation across the CTG, then the fermions emit or absorb two magnons (one by each fermion) with momenta \mathbf{q} and $-\mathbf{q}$ before recombining by emitting an outgoing photon with the energy $\omega_f = \omega_i - \omega$. The internal frequency integral of the corresponding diagram has three denominators [see Fig. 2(b) and Eq. (5) in Ref. 27] that could vanish simultaneously for a certain region of ω_i and ω_f . If the conditions for simultaneous vanishing of all three denominators are satisfied, this process gives a resonant RS enhancement known as *triple resonance*.³³ The *triple resonance* enhancement conditions depend on the dispersion of the fermionic bands and of the magnons. They have been calculated in Ref. 27 for the one-band Hubbard model within the spin-density wave (SDW) formalism, where the excitations between lower and upper Hubbard bands separated by U correspond to excitations across the CTG. These excitations produce both the spin exchange constant J and the 2M resonant RS vertex. That model description of the electronic states at half filling predicts no *triple resonance* conditions for excitation frequencies ω_i around the CTG energy 2Δ . The enhancement for Raman shifts ω between ~ 2.4 and $4J$ occurs twice: first

when ω_i lies between ~ 2.4 and $5.6J$ above 2Δ and second, even stronger, when ω_i approaches the upper edge of the electron-hole excitation band (see Fig. 3 in Ref. 27).

This *triple resonance* process can explain each of the observed features (a)–(d):

(a) The *triple resonance* contributes to all three experimentally observed scattering symmetries: B_{1g} , A_{1g} , and B_{2g} .

(b) The largest contribution from *triple resonance* scattering is in the B_{1g} channel, where, due to the geometric form factor for magnon emission, mainly short wavelength magnons from the vicinity of the magnetic Brillouin zone boundary participate in the process. The 2M density of states from the vicinity of these points diverges at the maximum 2M energy $4J$. Accounting for the final state interaction leads to partial renormalization of the 2M spectral weight^{5–8} and shifts the maximum of the 2M spectral weight down to $\sim 2.8J$. As a result, the observed 2M line shape (see Fig. 1) consists of two peaks: one is close to $4J$, and the other, due to magnon-magnon scattering, is at about $2.8J$ ($J_{\text{SCOC}} \approx 130$ meV, $J_{\text{YBCO}} \approx 110$ meV).³⁴ The relative intensity of these two peaks depends on the *triple resonance* conditions.

(c) In the A_{1g} channel the long wavelength magnons from the vicinity of the magnetic Brillouin zone center contribute to 2M scattering and determine the cubic polynomial low-frequency slope of the 2M line shape³⁵ for $\text{Sr}_2\text{CuO}_2\text{Cl}_2$. The threshold at about 1750 cm^{-1} in the 2M intensity observed for $\text{YBa}_2\text{Cu}_3\text{O}_{6+\delta}$ could be related to interlayer superexchange J_{\perp} within the CuO_2 -plane bilayers: the interlayer coupling results in an optical magnon branch with a gap of $2\sqrt{JJ_{\perp}}$ (Ref. 36) and an onset for 2M intensity at $4\sqrt{JJ_{\perp}}$ (Ref. 35). Experimentally, however, neither 2M RS line shape nor inelastic neutron scattering³⁶ have shown clear signature of the optical mode. Instead, Raman spectra at low energies show a flat continuum that could be result of strong fermionic damping of magnetic excitations across the optical gap, or incoherence within the double layers. For higher energies ($\omega > 1750$ cm^{-1}) the 2M line shape shows the expected cubic polynomial. This energy value gives an estimate for the energies where acoustic and optical magnon branches get close and hence we obtain $J_{\perp} \lesssim J/4$.

(d) The *triple resonance* theory predicts two peaks for the RREP at $\omega = 2.8J$: the first one at $\omega_i = \omega_i^{\text{res1}} \approx 2\Delta + 2.9J$, and the second at ω_i^{res2} , almost at the upper edge of the electron-hole excitation band. This prediction correlates with observed features (see Fig. 2), where the first resonance is about 2.9 – $3.4J$ above 2Δ , and the RREP shows a strong rise to the second resonance. Moreover, the model calculation of the Raman vertex in the absence of damping predicts that the 2M peak intensity increases by an inverse linear law as the incoming photon energy approaches the upper edge of the charge-transfer excitation band. In the inset of Fig. 2 we display the satisfactory linear fit of the inverse 2M intensity data for $\text{YBa}_2\text{Cu}_3\text{O}_{6+\delta}$ versus ω_i and extract the linear singularity excitation energy $\omega_i^{\text{res2}} \approx 3.1$ eV. The latter allows one to estimate the electron-hole excitation band width as $\omega_i^{\text{res2}} - 2\Delta \approx 1.3$ eV and nearest-neighbor hopping integral $t_{\text{YBCO}} \approx 320$ meV since $\omega_i^{\text{res2}} \approx 2\sqrt{\Delta^2 + 16t^2}$.

Our analysis has been based on the *triple resonance* calculations^{8,27} that have used a simplified effective one-band Hubbard model mapped on SDW formalism and only nearest-neighbor hopping integrals t have been taken into account. By breaking electron-hole symmetry, the Hubbard model with next-nearest-neighbor hopping t' (Ref. 37) already provides satisfactory agreement between the narrow (≈ 0.3 eV) valence band width observed in photoemission experiments³⁸ and our estimate (≈ 1.3 eV) for the sum of the valence and conduction bands width. Accounting for t' also results in a different strength and position of the *triple resonance* at $\omega_i^{\text{res}1}$ in the two investigated AF's, but does not effect $\omega_i^{\text{res}2}$ and our estimate of the hopping integral t (Ref. 39). Within the more realistic three band Hubbard model, there are excitations between the $2p_\sigma$ oxygen band and the upper Hubbard $3d(x^2-y^2)$ copper band, with CTG ϵ_{dp} , and excitations between lower and upper Hubbard bands, with a larger gap $\approx 2\epsilon_{dp}$. Both excitations contribute to the spin (super)exchange,⁴⁰ but only the $p \rightarrow d$ transition contributes to the resonant RS for $\omega_i \lesssim 3$ eV. For these lower excitation energies the three-band Hubbard problem can be mapped onto an effective one-band Hubbard model with ϵ_{dp} playing the role of U .

In summary, we have performed low-temperature two-magnon RREP measurements for single-layer $\text{Sr}_2\text{CuO}_2\text{Cl}_2$

and bilayer $\text{YBa}_2\text{Cu}_3\text{O}_{6+\delta}$ AF insulators over almost the entire region of electron-hole excitations across the CTG. We have shown that the experimental data are in general agreement with the theory proposed by Chubukov and Frenkel,^{8,27} indicating that the *triple resonance* process gives the leading contribution to resonant 2M scattering. This process contributes to B_{1g} , A_{1g} , and B_{2g} scattering geometries. The B_{1g} 2M line shape is composite and contains two peaks at about 2.8 and $4J$. The intensities of the two peaks strongly depend on the excitation resonance conditions. By measuring the excitation energy of the *triple resonance* $\omega_i^{\text{res}2}$ and knowing the CTG from the optical conductivity, we estimate the electron-hole excitation band width to be ≈ 1.3 eV and the nearest-neighbor hopping integral $t_{\text{YBCO}} \approx 320$ meV. The A_{1g} 2M line shape of bilayer $\text{YBa}_2\text{Cu}_3\text{O}_{6.1}$ material gives an estimate for the upper limit of interlayer superexchange $J_\perp \lesssim J/4$.

We are indebted to A. V. Chubukov and D. M. Frenkel for many valuable discussions. This work was supported by NSF Grant No. DMR 93-20892 (G.B., P.A., M.V.K.), cooperative agreement DMR 91-20000 through the STCS (G.B., M.V.K., W.C.L., D.M.G.), NSF Grant No. DMR 94-03894 (A.Z.), and DOE Grant No. W-7405-Eng82 through Ames Laboratory, ISU (L.L.M.).

*Present address: Department of Physics, Sook-Myung Women's University, Seoul, Korea.

¹D. Vagnin *et al.*, Phys. Rev. Lett. **58**, 2802 (1987); J. M. Tranquada *et al.*, *ibid.* **60**, 156 (1988); J. M. Tranquada *et al.*, Phys. Rev. B **40**, 4503 (1989).

²G. Shirane *et al.*, Phys. Rev. Lett. **59**, 1613 (1987).

³B. S. Shastry and B. I. Shraiman, Phys. Rev. Lett. **65**, 1068 (1990); Int. J. Mod. Phys. B **5**, 365 (1991).

⁴P. A. Fleury and R. Loudon, Phys. Rev. **166**, 514 (1968).

⁵R. J. Elliott and M. F. Thorpe, J. Phys. C **2**, 1630 (1969); J. B. Parkinson, *ibid.* **2**, 2012 (1969).

⁶R. R. P. Singh, Comments Condens. Matter Phys. **15**, 241 (1991).

⁷C. M. Canali and S. M. Girvin, Phys. Rev. B **45**, 7127 (1992).

⁸A. V. Chubukov and D. M. Frenkel, Phys. Rev. B **52**, 9760 (1995).

⁹K. B. Lyons *et al.*, Phys. Rev. B **37**, 2353 (1988).

¹⁰S. Sugai *et al.*, Phys. Rev. B **38**, 6436 (1988).

¹¹Y. Tokura *et al.*, Phys. Rev. B **41**, 11 657 (1990).

¹²P. E. Sulewski *et al.*, Phys. Rev. Lett. **67**, 3864 (1991).

¹³K. B. Lyons *et al.*, Phys. Rev. Lett. **60**, 732 (1988).

¹⁴P. Knoll *et al.*, Phys. Rev. B **42**, 4842 (1990).

¹⁵M. Yoshida *et al.*, Phys. Rev. B **42**, 8760 (1990).

¹⁶I. Tomeno *et al.*, Phys. Rev. B **43**, 3009 (1991).

¹⁷S. Sugai and Y. Hidaka, Phys. Rev. B **44**, 809 (1991).

¹⁸G. Blumberg *et al.*, Phys. Rev. B **49**, 13 295 (1994).

¹⁹K. B. Lyons *et al.*, Phys. Rev. B **39**, 9693 (1989).

²⁰S. Sugai, Phys. Rev. B **39**, 4306 (1989).

²¹P. E. Sulewski *et al.*, Phys. Rev. B **41**, 225 (1990).

²²M. Yoshida *et al.*, Phys. Rev. B **46**, 6505 (1992).

²³R. Liu *et al.*, J. Phys. Chem. Solids **54**, 1347 (1993).

²⁴The RREP data reported in Ref. 23 for large ω_i is in error because of calibration difficulties.

²⁵M. Mayer *et al.*, Physica C **235-240**, 1097 (1994).

²⁶M. Rübhausen *et al.* (unpublished).

²⁷A. V. Chubukov and D. M. Frenkel, Phys. Rev. Lett. **74**, 3057 (1995).

²⁸J. P. Rice and D. M. Ginsberg, J. Cryst. Growth **109**, 432 (1991); W. C. Lee and D. M. Ginsberg, Phys. Rev. B **44**, 2815 (1991).

²⁹L. L. Miller *et al.*, Phys. Rev. B **41**, 1921 (1990).

³⁰J. Humlicek *et al.*, Solid State Commun. **67**, 589 (1988).

³¹A. Zibold *et al.* (private communication).

³²V. N. Denisov *et al.*, Phys. Rev. B **48**, 16 714 (1993).

³³M. Cardona, in *Light Scattering in Solids II*, edited by M. Cardona and G. Günterodt (Springer-Verlag, New York, 1982).

³⁴For the bilayer case the interlayer superexchange interaction J_\perp shifts these energies upwards by an amount J_\perp .

³⁵Dirk K. Morr *et al.* (unpublished).

³⁶J. M. Tranquada *et al.*, Phys. Rev. B **40**, 4503 (1989).

³⁷A. V. Chubukov and K. A. Musaelian, J. Phys. Condens. Matter **7**, 133 (1995).

³⁸B. O. Wells *et al.*, Phys. Rev. Lett. **74**, 964 (1995).

³⁹A. V. Chubukov (private communication).

⁴⁰H. Eskes and J. H. Jefferson, Phys. Rev. B **48**, 9788 (1993).